HAWC Study of UHE Spectrum of MGRO J1908+06

arXiv:2112.00674 [astro-ph.HE]

Group D - UHE Cosmic Rays

CERN Latin-American School of HEP 2023

Outline

---

1. Introduction and motivation
2. HAWC & MGRO J1908-06 data
3. Diffusion model
4. Statistics & results
5. Implications for multi-wavelength and multi-messenger experiments
6. Conclusions

Introduction

Cosmic Rays (CRs)

CR (CERN)

- High energy particles arriving from outer space → **Primary Cosmic Rays (PCR)**
  - **Hadronic** (*p-n*, *α*, *heavy* nuclei) & **γ-rays**
- **Secondary showers** generated upon collision with atmosphere constituents
- Shower properties depends on PCR nature
- Most of the shower does not reach ground level (i.e., mostly ***muons***)
- "Fixed-target" experiment: **atmosphere** as target

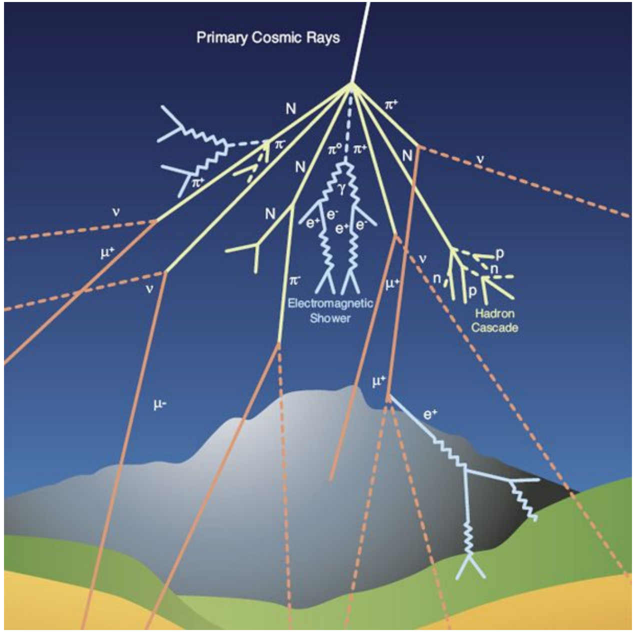

IceCube Masterclass

Ultra High Energy (UHE) CRs

- PCR energies vary between 10^{9}–10^{20} eV
- **UHECRs** → Energies greater than 10^{18} eV

- What sources can emit at these energies?
  - Galactic/extra-galactic
  - Neutron stars, pulsars
  - Supernovas, AGNs, etc.

- What are the **acceleration mechanisms**?

- Sufficient number of particles in secondary shower → Can be detected by **large arrays of ground detectors**

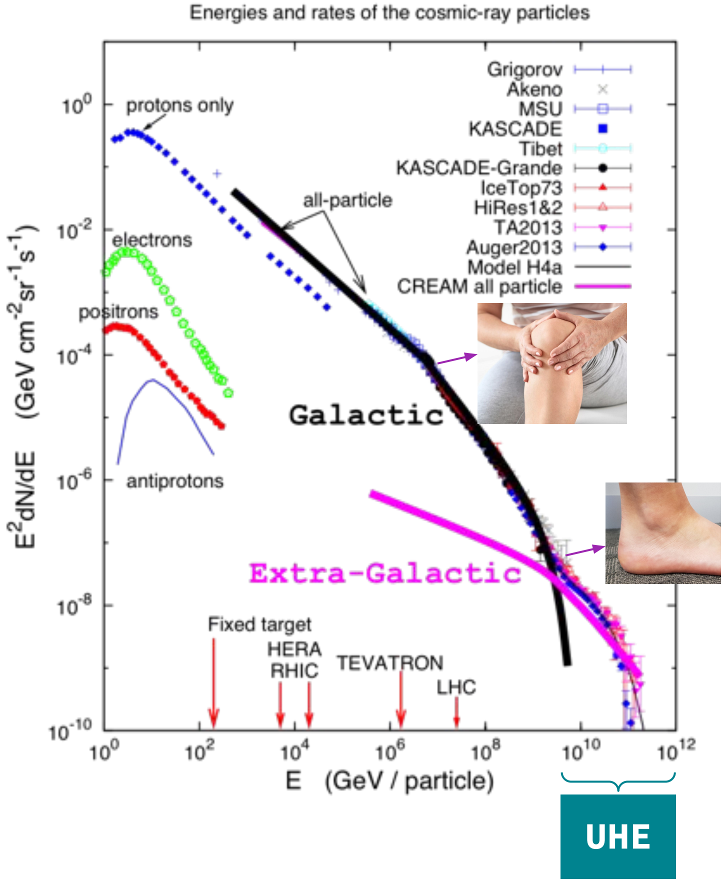

HAWC & MGRO J1908+06

High Altitude Water Cherenkov (HAWC) Observatory

2nd **generation** wide-field γ-ray detector

4100m altitude **(Sierra Negra, Puebla, México)**

22000 m^2 area, **300 tanks (WCDs) w/ 4 PMTs each**

4.5m in height and 7.3m in diameter

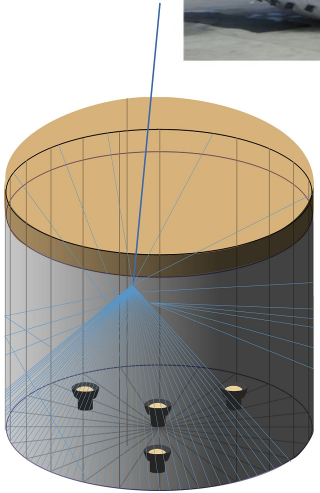

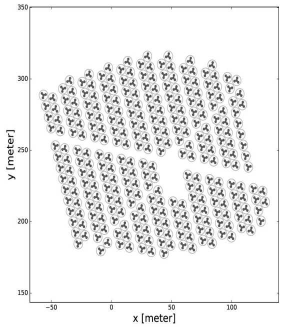

MGRO J1908+06 and HAWC dataset

- MGRO J1908+06
  - Discovered by MILAGRO
  - Emitting above 100 TeV

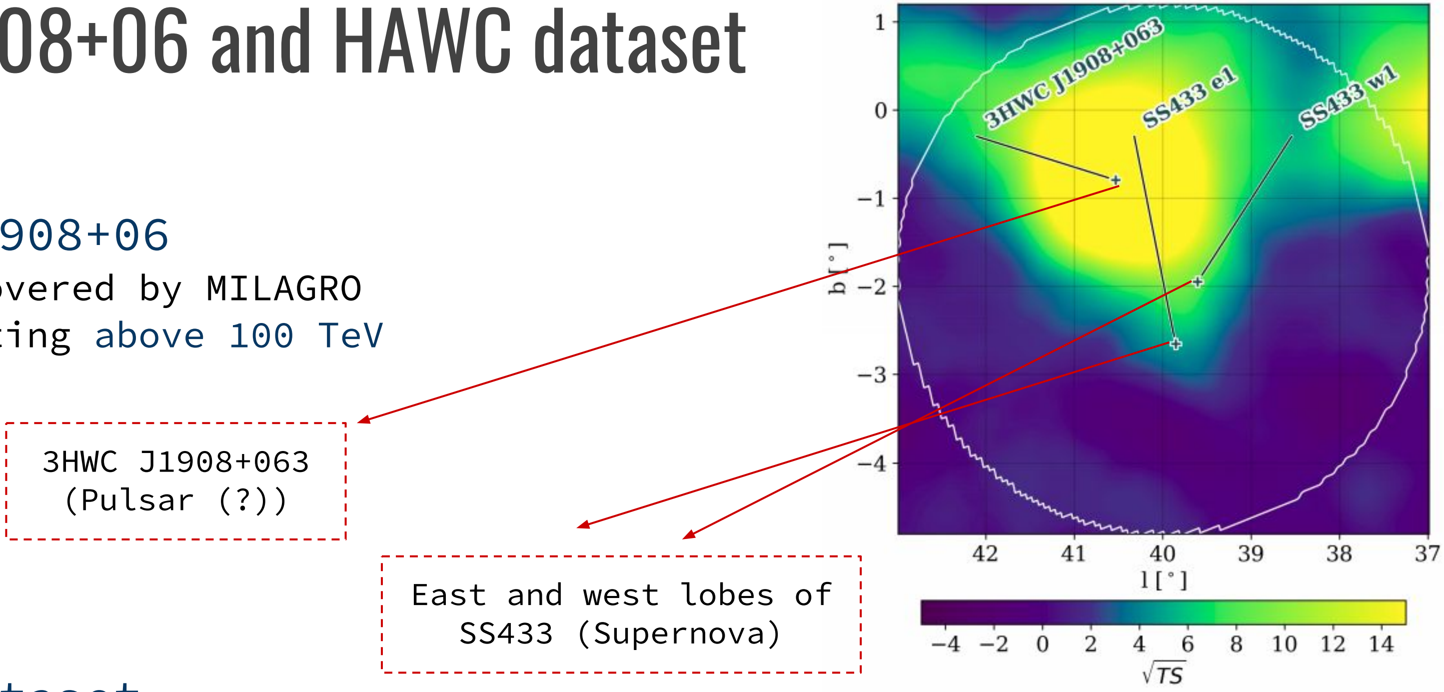

- HAWC dataset
  - 1343 days (June 2015-2019)
  - Binned 2D scheme
    - Estimated Energy (Ê) x fractional multiplicity

Diffusion Model

Diffusion Model

$$\frac{dN}{dE} = \phi_0 \left(\frac{E}{20\ \mathrm{TeV}} \right)^{-2.0}$$

Flux from east and west lobes of SS433

↓

Point sources

Fixed spectral indices

$$\frac{dN}{dE} = \phi_0 \left(\frac{E}{10\ \mathrm{TeV}} \right)^{-\alpha - \beta \ln(E/10\ \mathrm{TeV})}$$

Flux from 3HWC J1908+63

↓

Extended source

Log-parabolic function
α and β are free parameters

Diffusion Model

- Gamma ray spectrum and morphology → e^+e^- pairs diffusing

Spatial morphology:

$$\frac{dN}{d\Omega} = 1.22 \frac{\exp\left(-\theta^2/\theta_d^2(E)\right)}{\pi^{3/2}\,\theta_d(E)\left(\theta + 0.06\,\theta_d(E)\right)}$$

total flux

diffusion angle

angle from the source

gamma-ray energy

Free parameters of the models:

for 3HWC J1908+063 → **α, β, ϕ_0 and θ_d**

for lobes of SS433 → ϕ_0

Statistical Analysis & Results

Statistical Analysis

- Best-fit parameters obtained via Maximum Likelihood Fit

Significance:

- 3HWC J1908+063 → 43.9σ
- East & West lobes → 2.9σ and 3.9σ

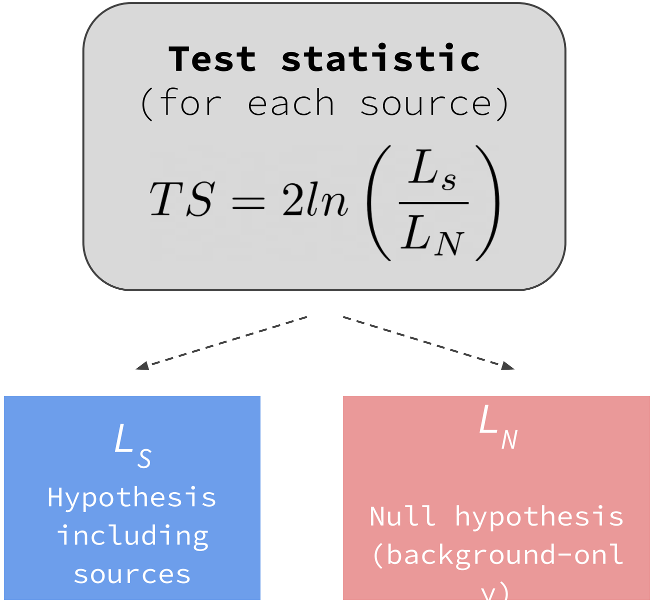

$\sqrt{(TS)}$ can be equated to Gaussian significance

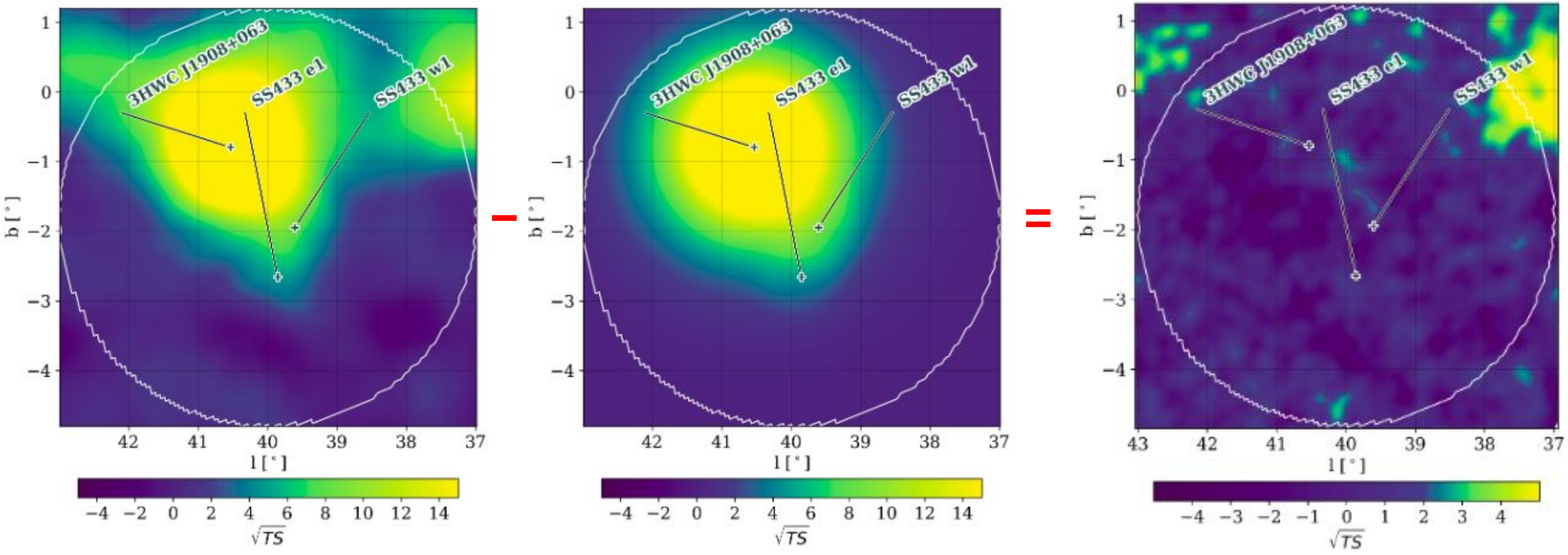

Left: HAWC significance map of the region.

Centre: Significance for the best fit model.

Right: Significance of the residuals (left-centre).

- Bulk of emission from 3HWC J1908+063
- Maximum significance of 38.8σ
- Residual centred at $l=37^0$, $b=0^0$ likely diffuse emission

Best-fit Model

Parameter	Best-fit value	Statistical uncertainty	Systematic uncertainty
θ_d	$1.78°$	$\pm 0.08°$	${}^{+0.07}_{-0.28}$
ϕ_0	1.17×10^{-13} (TeV cm^2 s)$^{-1}$	$\pm 0.06 \times 10^{-13}$ (TeV cm^2 s)$^{-1}$	${}^{+0.10}_{-0.23} \times 10^{-13}$ (TeV cm^2 s)$^{-1}$
α	2.545	± 0.026	${}^{+0.01}_{-0.06}$
β	0.134	± 0.018	${}^{+0.02}_{-0.03}$
ϕ_{SS433E}	2.0×10^{-16} (TeV cm^2 s)$^{-1}$	${}^{+1.0}_{-0.7} \times 10^{-16}$ (TeV cm^2 s)$^{-1}$	${}^{+0.2}_{-0.1} \times 10^{-16}$ (TeV cm^2 s)$^{-1}$
ϕ_{SS433W}	3.0×10^{-16} (TeV cm^2 s)$^{-1}$	${}^{+1.1}_{-0.8} \times 10^{-16}$ (TeV cm^2 s)$^{-1}$	${}^{+0.2}_{-0.6} \times 10^{-16}$ (TeV cm^2 s)$^{-1}$

- Assuming the distance to the source is that of 3HWC J1907+0602, the diffusion radius (r_d) of the particle is ~74 parsec

$$r_d = \frac{\pi}{180}\theta_d \; d_{src}$$

Best-fit Model

Parameter	Best-fit value	Statistical uncertainty	Systematic uncertainty
θ_d	$1.78°$	$\pm\, 0.08°$	${}^{+0.07}_{-0.28}$
ϕ_0	1.17×10^{-13} (TeV cm^2 s)$^{-1}$	$\pm\, 0.06 \times 10^{-13}$ (TeV cm^2 s)$^{-1}$	${}^{+0.10}_{-0.23} \times 10^{-13}$ (TeV cm^2 s)$^{-1}$
α	2.545	$\pm\, 0.026$	${}^{+0.01}_{-0.06}$
β	0.134	$\pm\, 0.018$	${}^{+0.02}_{-0.03}$
ϕ_{SS433E}	2.0×10^{-16} (TeV cm^2 s)$^{-1}$	${}^{+1.0}_{-0.7} \times 10^{-16}$ (TeV cm^2 s)$^{-1}$	${}^{+0.2}_{-0.1} \times 10^{-16}$ (TeV cm^2 s)$^{-1}$
ϕ_{SS433W}	3.0×10^{-16} (TeV cm^2 s)$^{-1}$	${}^{+1.1}_{-0.8} \times 10^{-16}$ (TeV cm^2 s)$^{-1}$	${}^{+0.2}_{-0.6} \times 10^{-16}$ (TeV cm^2 s)$^{-1}$

- Assuming the distance to the source is that of 3HWC J1907+0602, the diffusion radius (r_d) of the particle is ~74 parsec

$$r_d = \frac{\pi}{180}\theta_d \; d_{src}$$

The HAWC Spectrum of 3HWC J1908+063

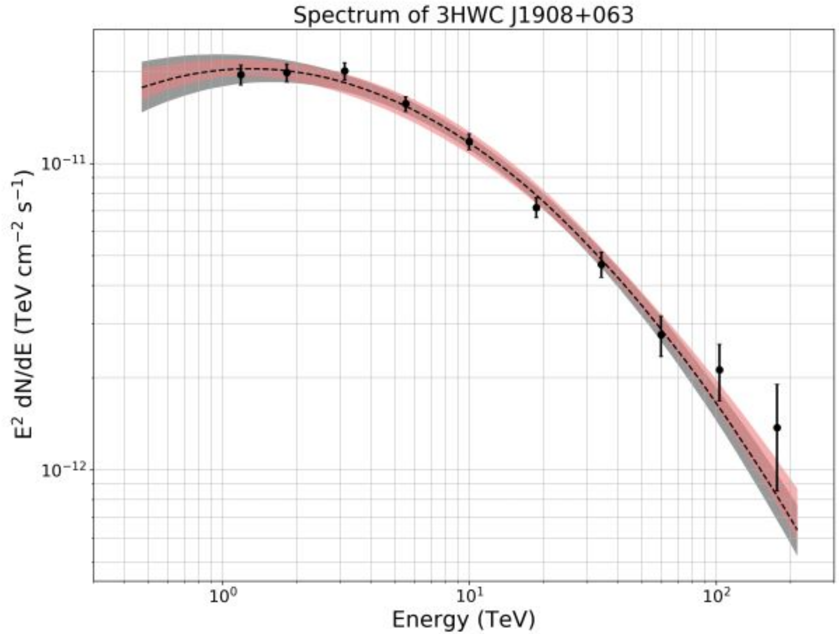

Systematic uncertainties width (pink band) range from ~+14%/-11% at 1 TeV to ~+20%/-11% at 100 TeV

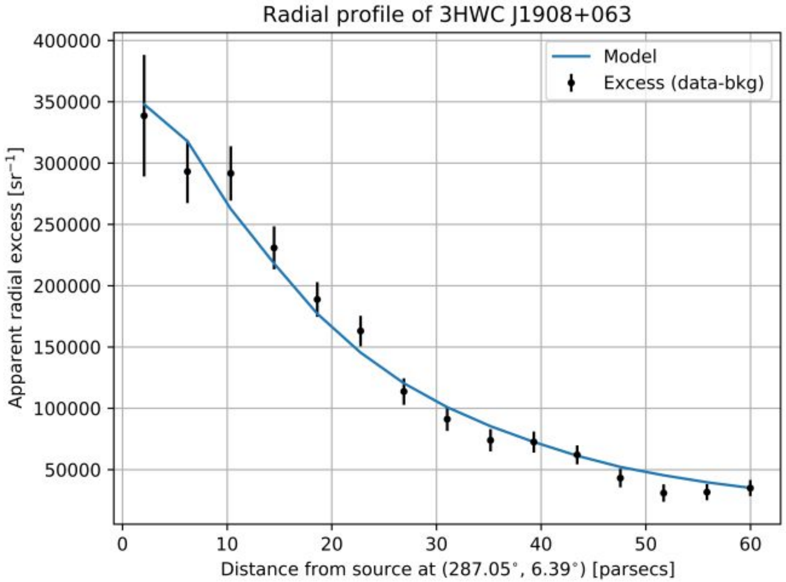

Consistent with particles diffusing from a source

Comparison with Other Experiments

Different:

- Source morphology
- Field of view
- Resolution
- Reconstruction techniques
- Background determination

➩ Good agreement with LHAASO experiment 😉

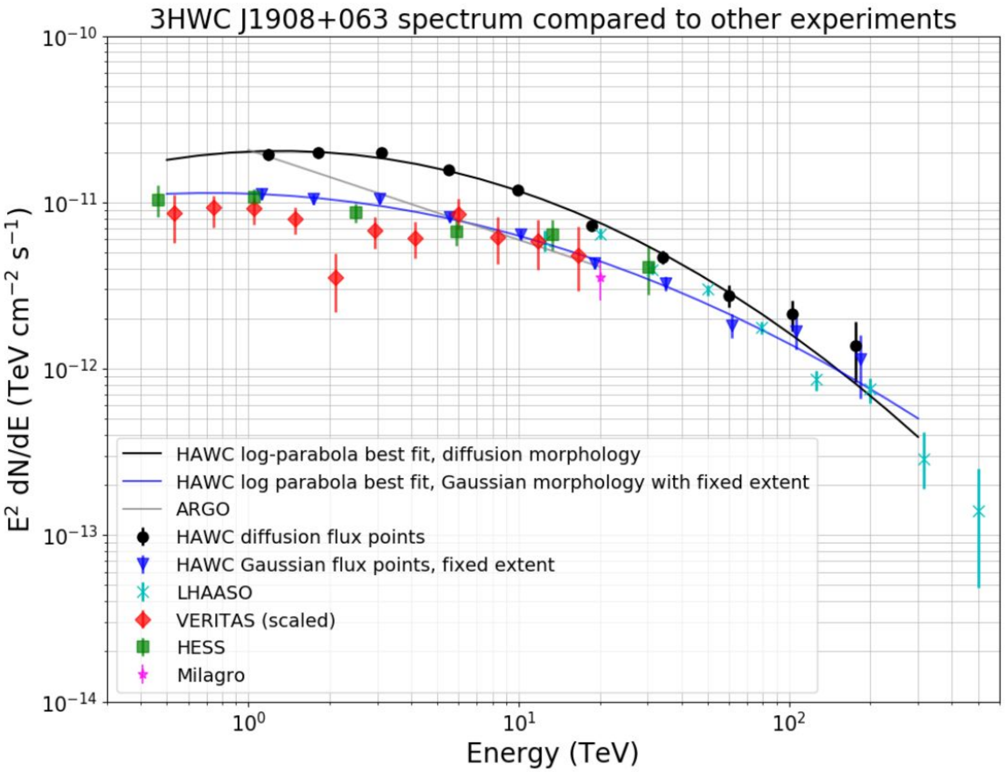

Comparison with Other Experiments

Different:

- Source morphology
- Field of view
- Resolution
- Reconstruction techniques
- Background determination

➩ Good agreement with LHAASO experiment 😉

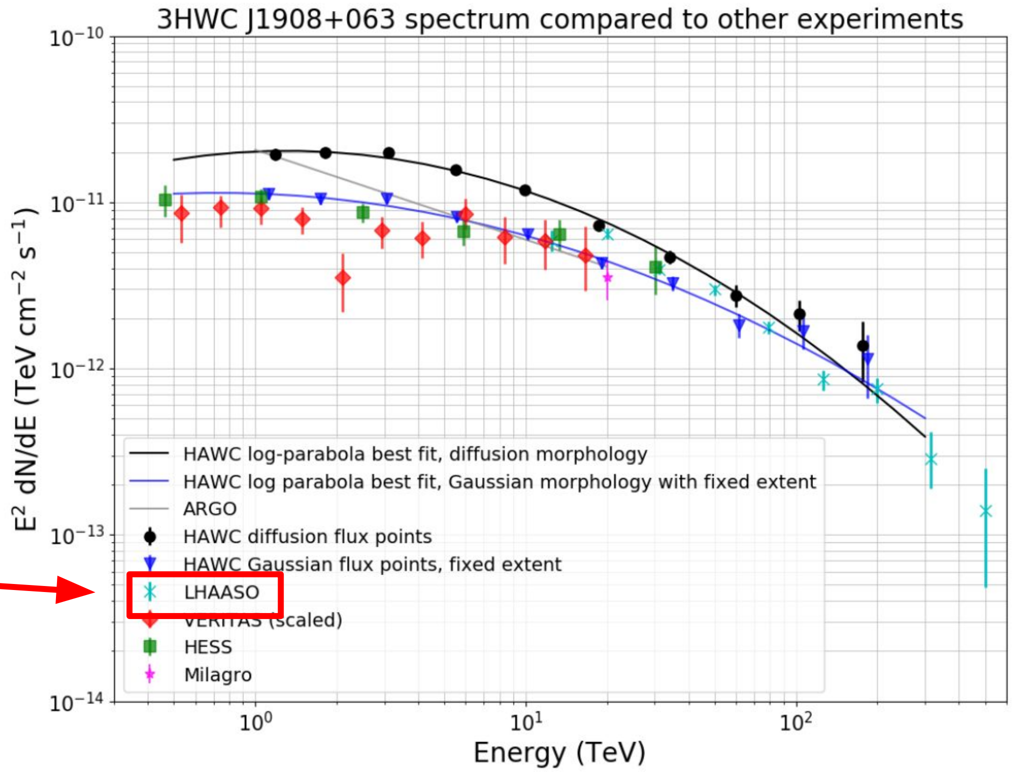

Theoretical Model

Methods of Production

Hadronic

- Pions produced in spallation reactions

$$\pi^0 \to \gamma\gamma$$

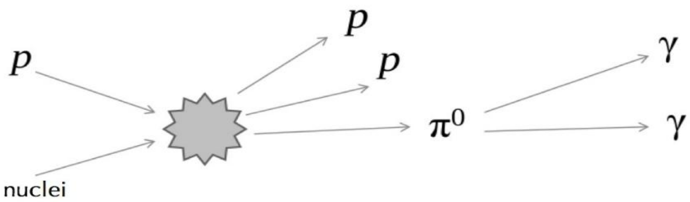

Leptonic

- Inverse Compton emission

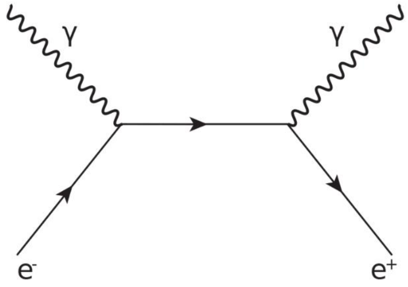

- Synchrotron emission

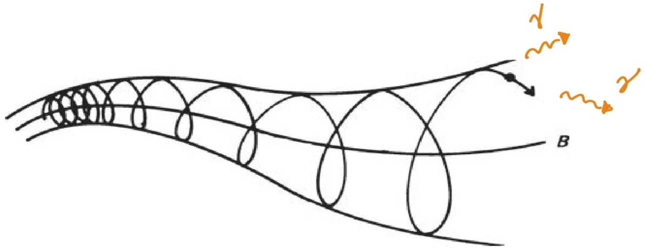

Possible Scenarios and Comparison with Data

1. Single hadronic source

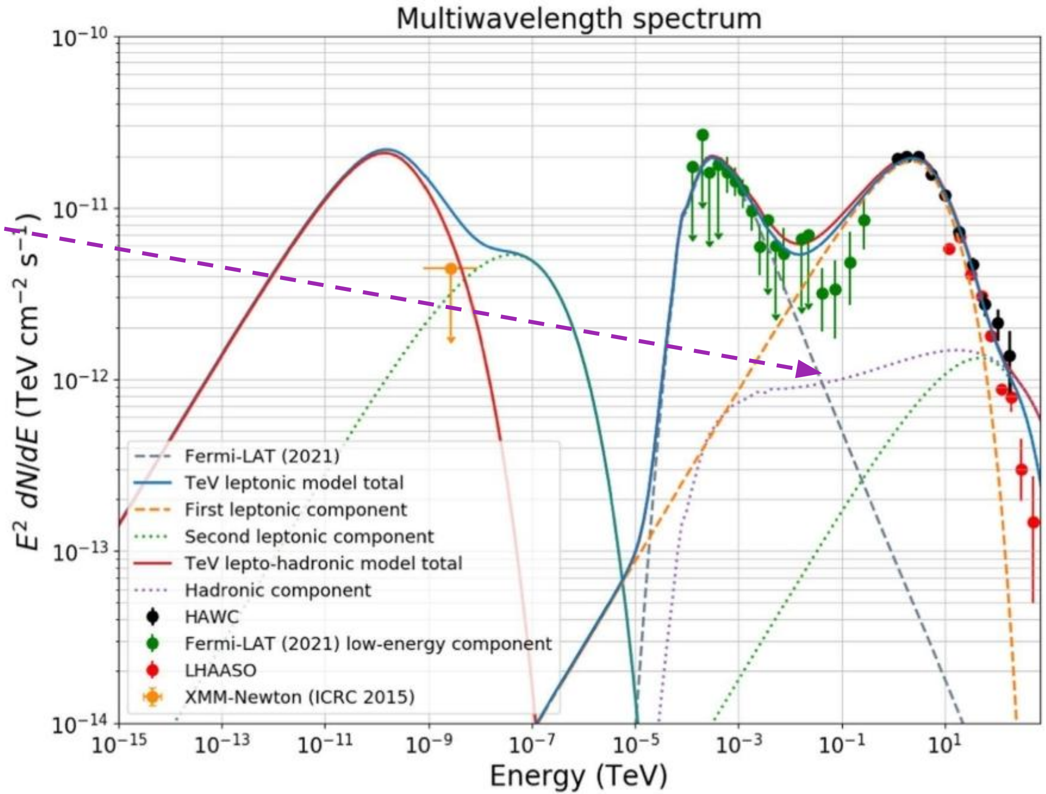

Possible Scenarios and Comparison with Data

1. Single hadronic source
2. Single leptonic source

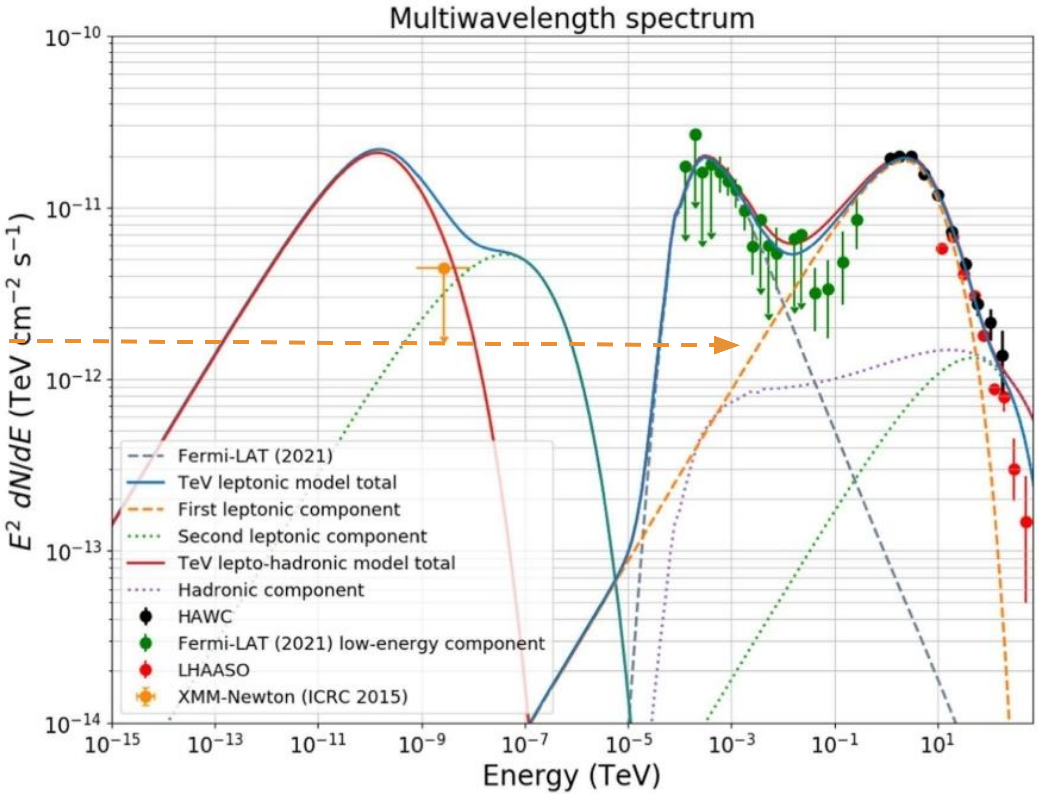

Possible Scenarios and Comparison with Data

1. Single hadronic source
2. Single leptonic source
3. Two leptonic components

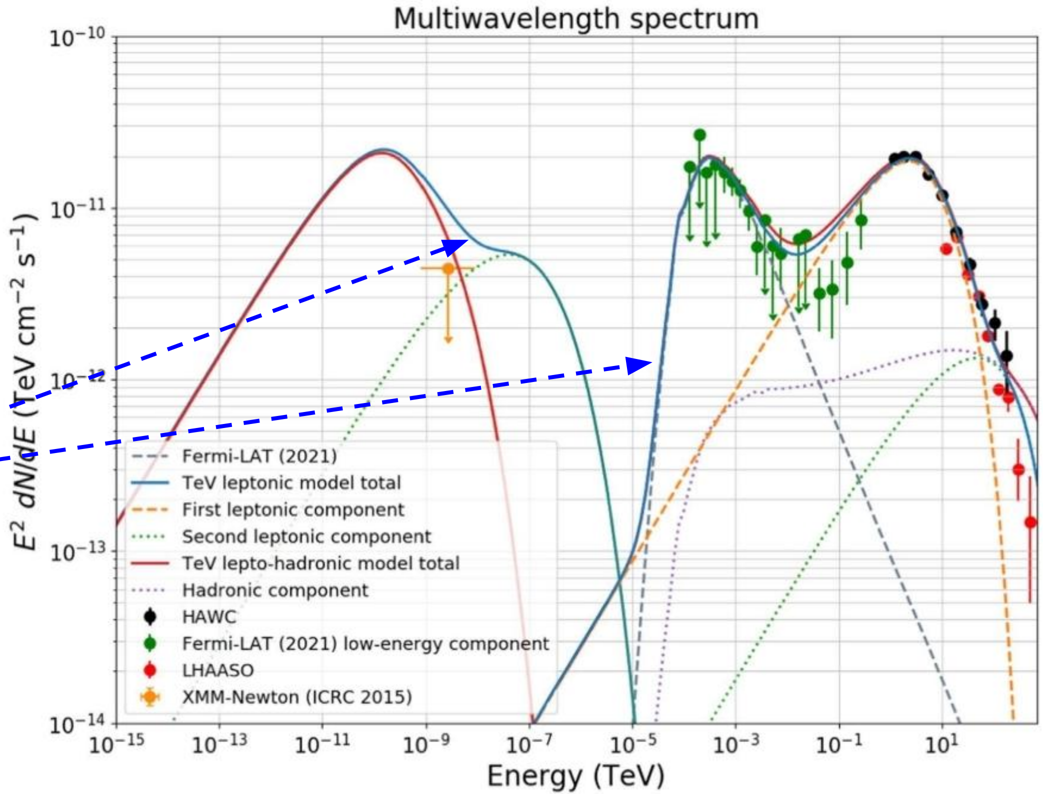

Possible Scenarios and Comparison with Data

1. Single hadronic source
2. Single leptonic source
3. Two leptonic components
4. Leptonic + Hadronic components

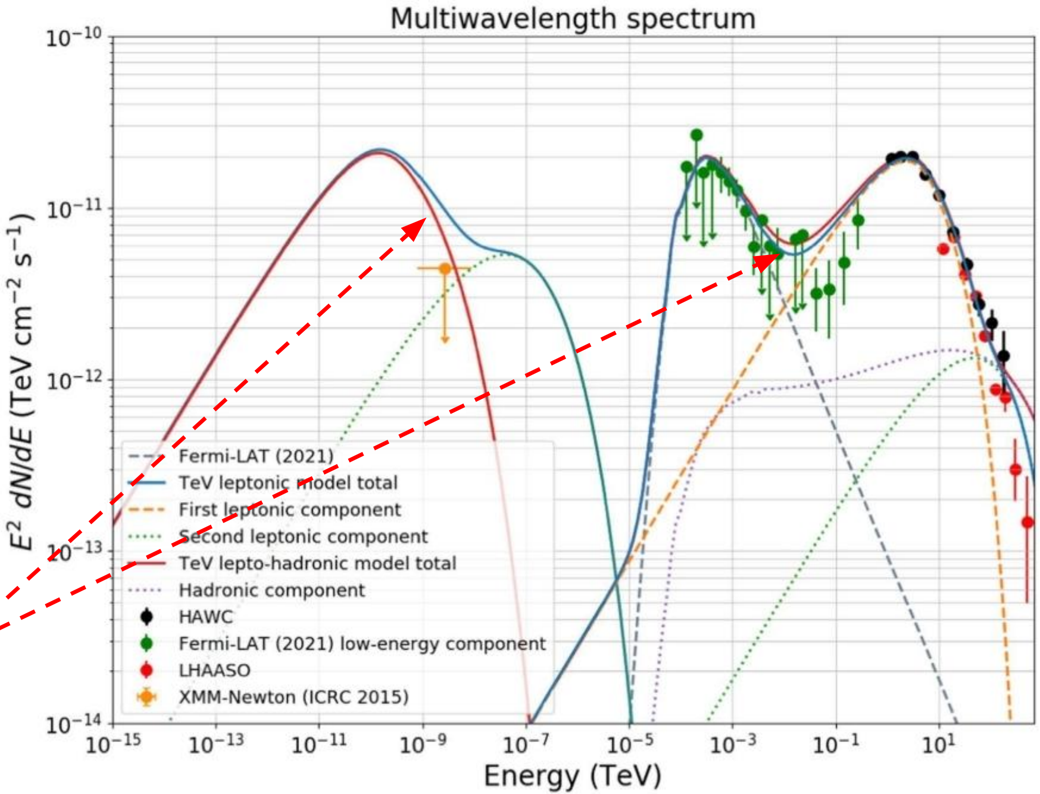

Possible Scenarios and Comparison with Data

1. Single hadronic source
2. Single leptonic source
3. Two leptonic components
4. Leptonic + Hadronic components

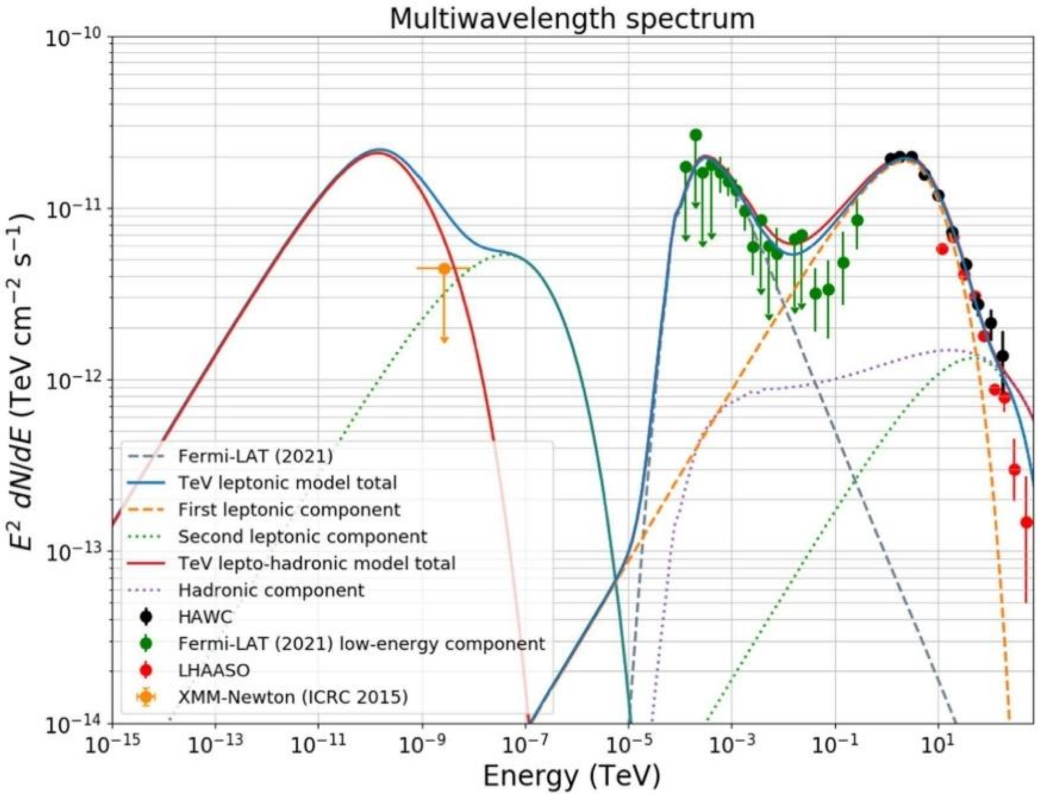

inconclusive results 😞

Implications for Multi-Wavelength and Multi-Messenger Experiments

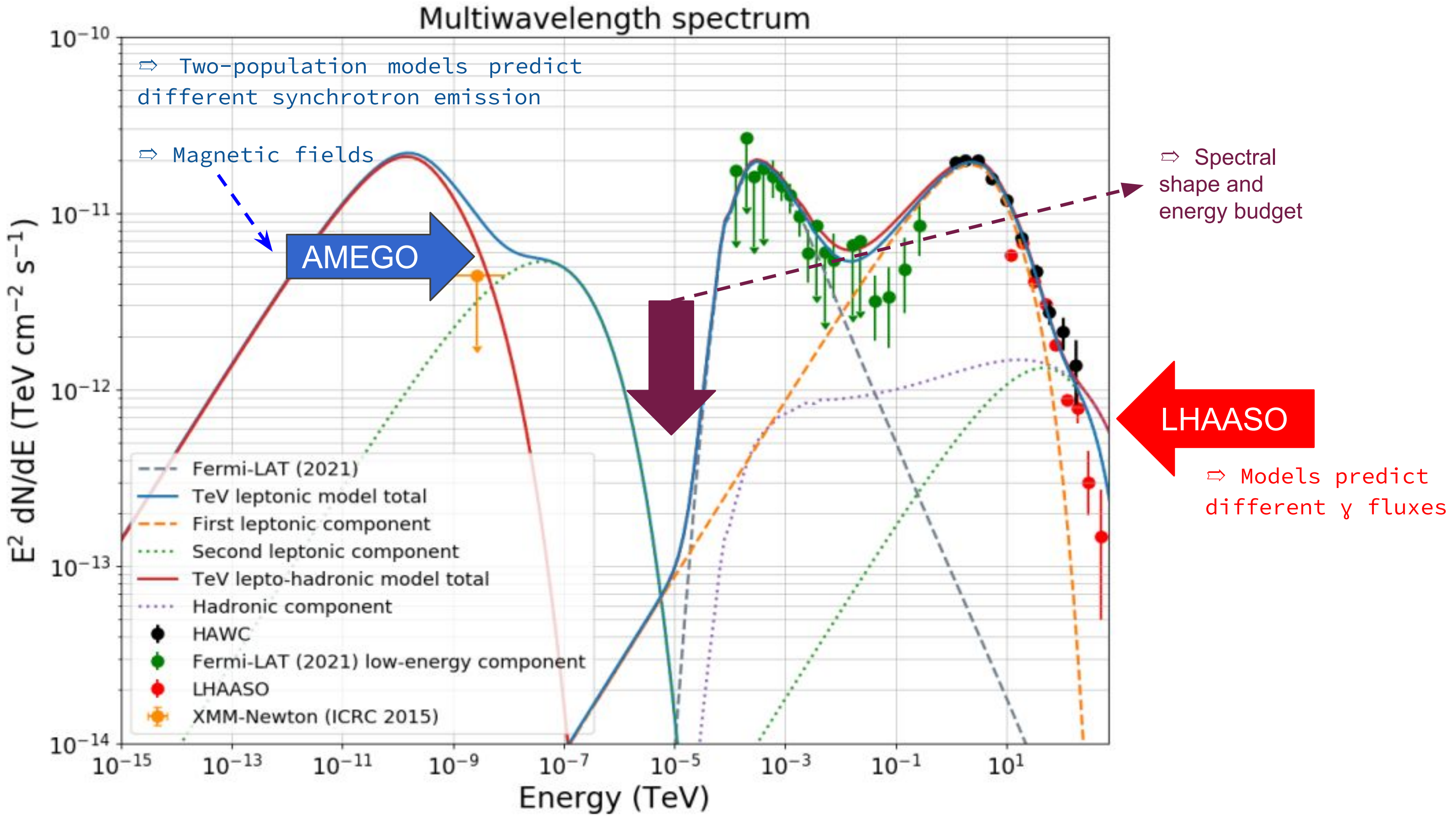

Multiwavelength spectrum
⇨ Two-population models predict different synchrotron emission
⇨ Magnetic fields
AMEGO
⇨ Spectral shape and energy budget
LHAASO
⇨ Models predict different γ fluxes
Fermi-LAT (2021)
TeV leptonic model total
First leptonic component
Second leptonic component
TeV lepto-hadronic model total
Hadronic component
HAWC
Fermi-LAT (2021) low-energy component
LHAASO
XMM-Newton (ICRC 2015)
E² dN/dE (TeV cm⁻² s⁻¹)
Energy (TeV)

Relation between a γ-ray flux and the corresponding ν-flux

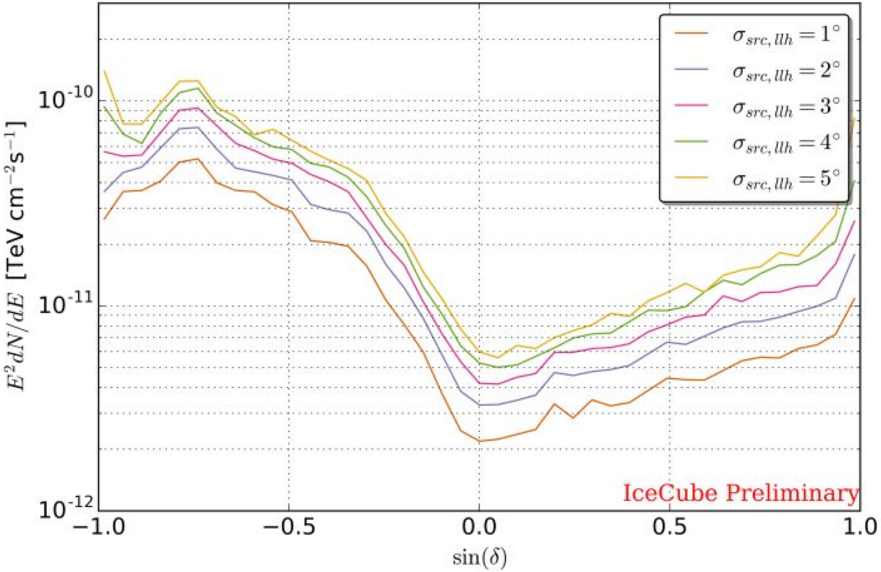

10% hadronic component prediction one order of magnitude below current IceCube discovery potential

PoS(ICRC2017)963

arXiv:2008.04323

Conclusions and Final Remarks

- **3HWC J1908+063** ➜ one of the few sources observed to emit in the TeV range
- **Source** consistent with **diffusion model** (extended)
- **Leptonic models** (one-two pop. & mixed with **hadronic**) consistent with data
    - Highly unconstrained parameter space
- In mixed scenario, **hadronic** contribution ➜ most important at highest energies
- Multi-messenger/wavelength observations will be important to **distinguish** between these **two contributions**

Conclusions and Final Remarks

- **3HWC J1908+063** ➜ one of the few sources observed to emit in the TeV range
- **Source** consistent with **diffusion model** (extended)
- **Leptonic models** (one-two pop. & mixed with **hadronic**) consistent with data
  - Highly unconstrained parameter space
- In mixed scenario, **hadronic** contribution ➜ most important at highest energies
- Multi-messenger/wavelength observations will be important to **distinguish** between these **two contributions**
- ~93% of our group didn't have (much/any) experience in the topic but we **survived**!!! 💪

Thank you! Gracias! Obrigado! Grazie!

BACK UP

HAWC & MGRO J1908+06

Trigger & Data Acquisition

- Time-over-threshold (**ToT**)
  - To determine the total charge collected in the PMT
- Noise:
  - **PMT afterpulsing, dark noise**
- Data Acquisition System (**DAQ**):
  - 1.5 µs of data from all PMTs hit
- Hits between -150 and +400 ns around trigger
- Real-time trigger based on **PMT hit multiplicity**
  - Events that hit few PMTs are usually discarded
  - Trigger air shower events at ~25 kHz

PMT signal

↓

Discriminators

↓

Time-to-digital converters (TDCs)

↓

Computer farms

Ground Parameter Estimator (I)

- Charge density at fixed distance to shower axis
  - Lateral distribution function (LDF)
  - Modified NKG function fit to the LDF → measure the **energy density**

PMT signal (charge)

shower age

distance of PMT to the shower axis

$$\log_{10}(sig_r) = A + s\left[\log_{10}\frac{r}{r_m} + \log_{10}\left(1+\frac{r}{r_m}\right)\right] - 3\log_{10}\frac{r}{r_m} - 4.5\log_{10}\left(1+\frac{r}{r_m}\right).$$

logarithm of the amplitude of the source

Móliere radius

Ground Parameter Estimator (II)

- **Energy is then obtained at 40m:**

$$\log_{10} \hat{E} = m(\theta) \log_{10} sig_{40} + c(\theta)$$

$m(\theta)$: **piecewise linear function**

$c(\theta)$: **piecewise quadratic function**

Water Cherenkov Detectors

- Light travelling through a transparent medium slows down according to the refractive index
  - Speed of light in water ~0.75c
- Charged particles faster than light in a medium:
  - Production of **light cone** (Cherenkov radiation)
- Cherenkov radiation is detected by PMTs and the cone of emission reconstructed
  - Cone’s axis gives the **direction of the particle**
  - The light intensity gives the **particle energy**

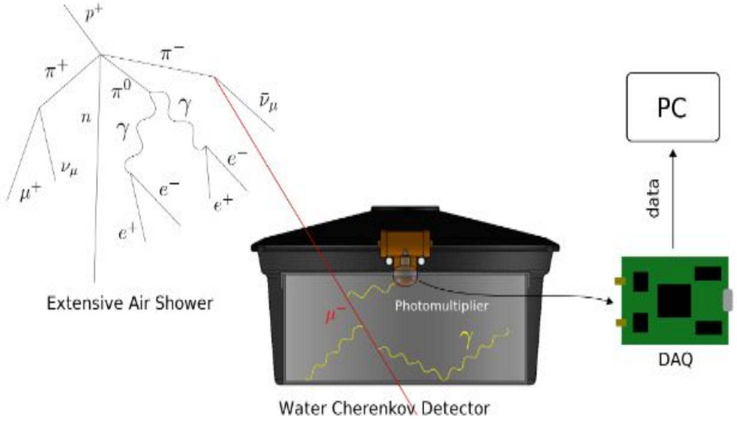

Statistical Analysis & Results

Systematics: Galactic Diffuse Emission

- Possible **galactic** diffusion:
  - Modelled as gaussian centered at $b=0^0$.
- β is lowered by ~16%
- Effect on the flux decreases with energy (varies between 18% and 31%)

Parameter	Galaxy	3HWC1908+063
Normalization $(\mathrm{TeV\,cm^2\,s})^{-1}$	$(1.9 \pm 0.4) \times 10^{-14}$	$(0.96 \pm 0.08) \times 10^{-13}$
$\sigma(^o)$	0.64 ± 0.15	—
$\theta_D(^o)$	—	1.50 ± 0.10
α	2.75 (fixed)	2.505 ± 0.032
β	—	0.150 ± 0.022

Theoretical Model

Theoretical Model

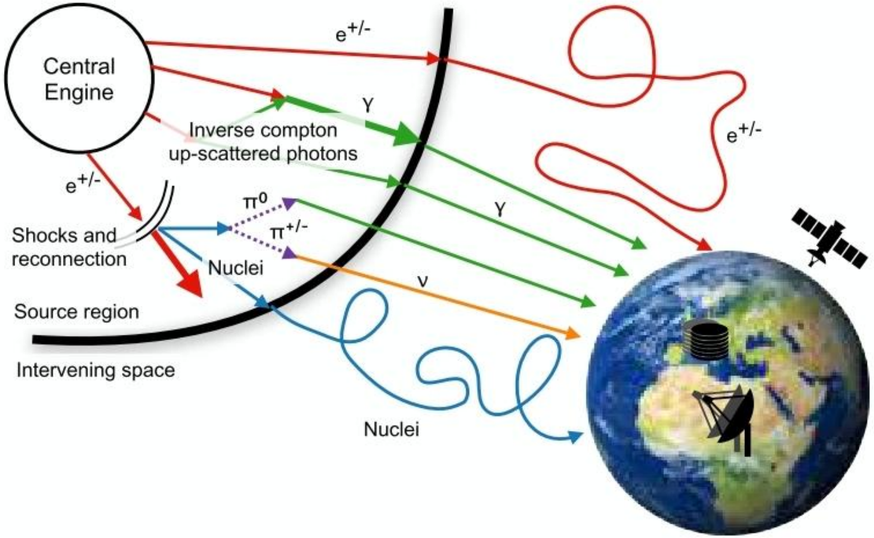

Implications for Multi-Wavelength and Multi-Messenger Experiments

Relation between a γ-ray flux and the corresponding ν-flux

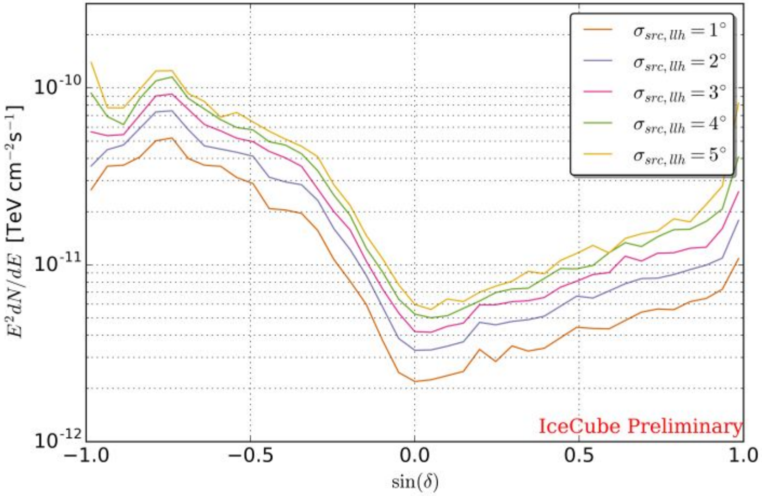

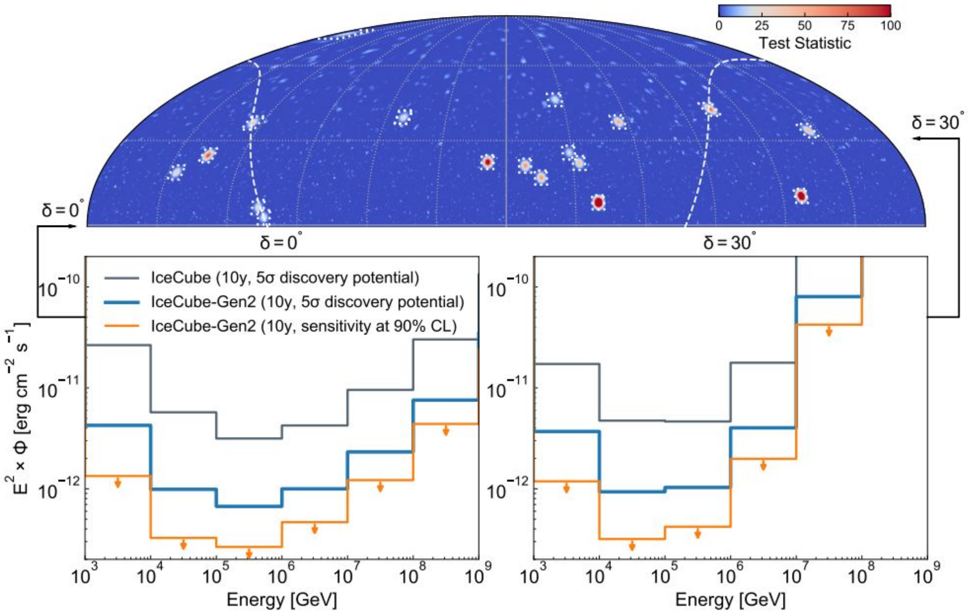

10% hadronic component prediction one order of magnitude below current IceCube discovery potential.

PoS(ICRC2017)963
2008.04323

Conclusions and Final Remarks

- Observations of UHE source 3HWC J1908+063 emitting to at least 200 TeV
- **Source** modelled using **electron diffusion model**
- Potential spectral hardening observed at highest energies
    - More data needed to test this hypothesis
- Leptonic models (one-two pop. & mixed with hadronic) consistent with data
    - Highly unconstrained parameter space
- In mixed scenario, hadronic contribution is most important at highest energies
- Fully hadronic origin unlikely for TeV gamma-ray emissions
- Multi-messenger/wavelength observations will be important to distinguish between these two contributions